Angewandte Chemie
Eine Zeitschrift der Gesellschaft Deutscher Chemiker

Supporting Information

69451 Weinheim, Germany

Origin of Low CO_2 Selectivity on Platinum in the Direct Ethanol Fuel Cell**

Richard Kavanagh, Xiao-Ming Cao, Wen-Feng Lin, Christopher Hardacre, and P. Hu**

anie_201104990_sm_miscellaneous_information.pdf

Supporting Information

1. Computational Details

All calculations reported here were carried out using the VASP package with the use of a plane wave basis set.[1-3] Electron exchange and correlation terms are described with the use of the generalised gradient approximation (GGA) using the PBE functional.[4] Electron-ion interactions are described using projector-augmented wave (PAW) potential.[5] The convergence of the plane-wave expansion was obtained using a cut-off energy of 400 eV. The two dimensional Brillouin integrations were fulfilled using a (5 x 5 x 1) Monkhorst-Pack grid.[6] The ground state was obtained using Methfessel-Paxton smearing of 0.05 eV.[7] Kinetic data was obtained using a constrained minimization transition state search technique.[8-10]
The monoatomic step was modelled as a (3 x 1 x 1) (2 1 1) unit cell. A slab of four layers was employed, with the upper two layers being relaxed and the lower two in fixed geometry. Separation of slabs in the normal direction was achieved using a vacuum region of 12 Å. The aqueous medium was modelled using Nose thermostat molecular dynamics simulations (T = 353 K, 0.5 fs/step, 6000 steps). For these calculations, the DFT-optimised surface species were fixed, while an initial ice-like water structure was allowed to relax. Following MD calculations, 6 configurations were randomly selected from the last 200 time-steps for each species and optimised by DFT, with the lowest-energy configuration being reported. In each case, the 6 calculated total energies were consistent to within 0.05 eV, demonstrating that the systems had reached an equilibrium state.

2. Kinetics

The formation of CO_2 and acetic acid initially share the same minimum energy pathway until the formation of $CH_3CO_{(ads)}$. This indicates that the elementary steps from ethanol to $CH_3CO_{(ads)}$ are not crucial to the selectivity between CO_2 and acetic acid. Starting from $CH_3CO_{(ads)}$, two parallel pathways yield CO_2 and acetic acid, respectively. Given that CO can be readily converted to CO_2 in the presence of water[11], either the dehydrogenation of $CH_3CO_{(ads)}$ to yield $CH_2CO_{(ads)}$ or the C-C bonding cleavage, *i.e.* $CH_2CO_{(ads)} \rightarrow CH_{2(ads)} + CO_{(ads)}$ is likely to be the key step in CO_2 formation. Comparing these two elementary steps, the energy barrier associated with C-C bond cleavage (0.90 eV) is higher than that associated with the dehydrogenation of $CH_3CO_{(ads)}$ (0.72 eV). This suggests that the C-C bond cleavage is the key step of CO_2 formation. It is expected that the coupling of $CH_3CO_{(ads)}$ and $OH_{(ads)}$ be the key step for acetic formation as it is a unique surface reaction step. Hence, the competition between C-C bond cleavage and the coupling of $CH_3CO_{(ads)}$ and $OH_{(ads)}$ determines the selectivity between CO_2 and acetic acid.

3. Intermediate and Transition State Structures and Bond Lengths (Å)

CH_3CH_2OH (ads)		
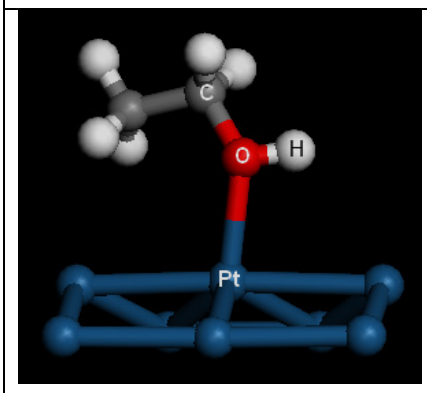	Pt – O	2.287
	C – O	1.461
	O – H	0.976
TS 1: CH_3CH_2OH (ads) → CH_3CHOH (ads)		
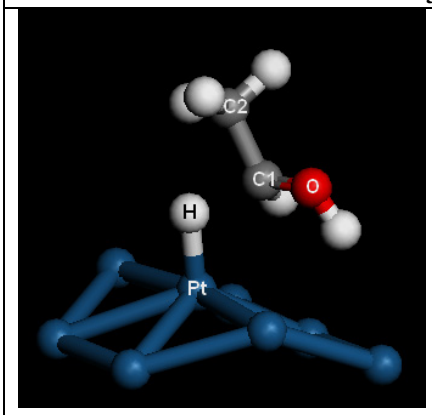	**C_1 – H**	**1.608**
	Pt – H	1.617
	Pt – C_1	2.461
	C_1 – C_2	1.505
	C_1 – O	1.358
CH_3CHOH (ads)		
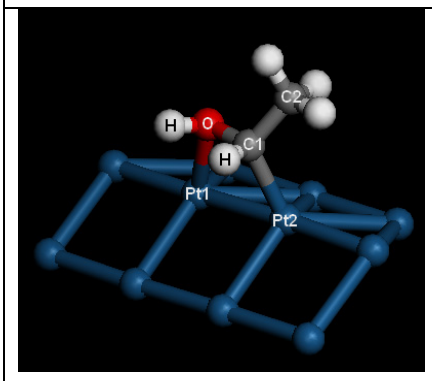	Pt_1 – O	2.292
	Pt_2 – C_1	2.056
	C_1 – C_2	1.510
	C_1 – O	1.483
	O – H_1	0.978
	C_1 – H_2	1.103
TS 2: CH_3CHOH (ads) → CH_3COH (ads)		
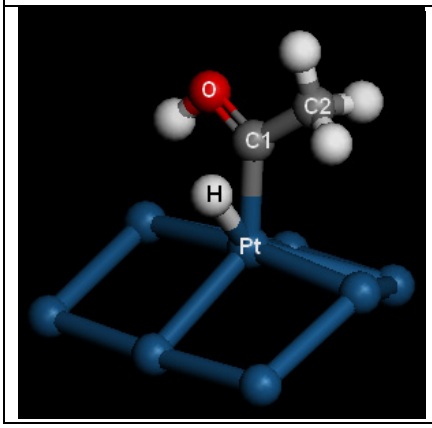	**C_1 – H**	**1.469**
	Pt – H	1.698
	Pt – C_1	1.973
	C_1 – C_2	1.491
	C_1 – O	1.327

CH_3COH (ads)		
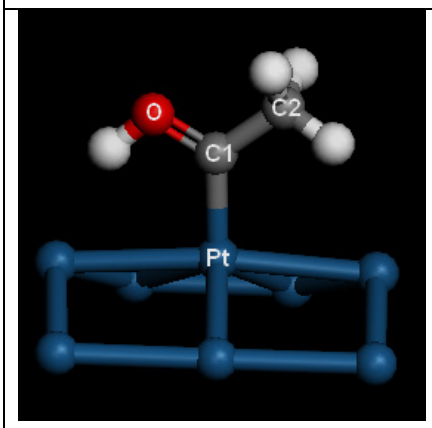	$Pt - C_1$	1.926
	$C_1 - C_2$	1.494
	$C_1 - O$	1.319
TS 3: CH_3COH (ads) ➔ CH_3CO (ads)		
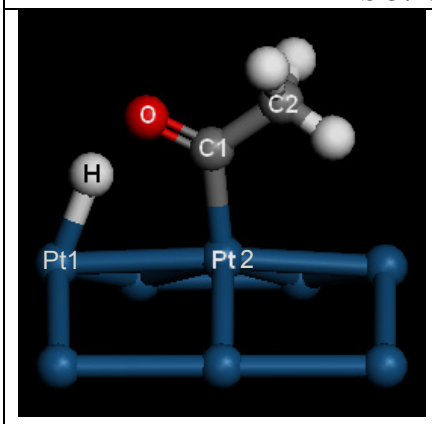	**O – H**	**1.424**
	$Pt_1 - H$	1.682
	$Pt_2 - C_1$	1.974
	$C_1 - C_2$	1.510
	$C_1 - O$	1.255
CH_3CO (ads)		
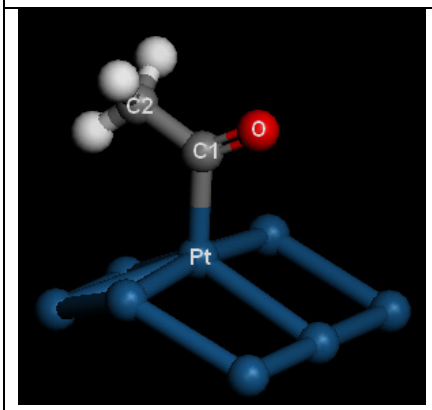	$Pt - C_1$	2.001
	$C_1 - C_2$	1.514
	$C_1 - O$	1.211
TS 4: CH_3CO (ads) ➔ CH_2CO (ads)		
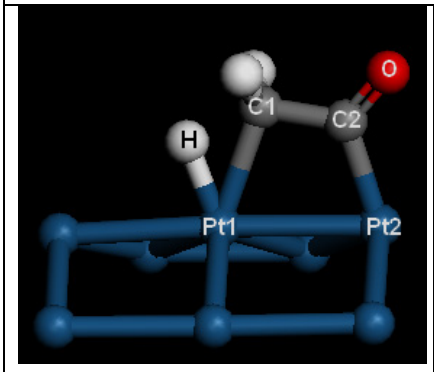	**$C_1 - H$**	**1.441**
	$Pt_1 - H$	1.624
	$Pt_1 - C_1$	2.249
	$Pt_2 - C_2$	1.980
	$C_1 - C_2$	1.533
	$C_2 - O$	1.214

CH_2CO (ads)		
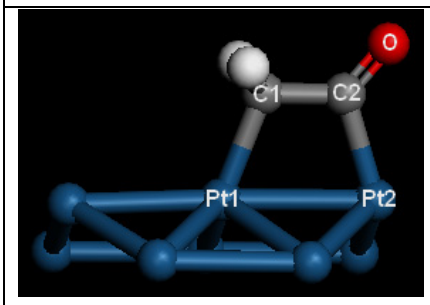	$Pt_1 - C_1$	2.070
	$Pt_2 - C_2$	2.005
	$C_1 - C_2$	1.499
	$C_2 - O$	1.207
TS 5: CH_2CO (ads) ➔ CH_2 (ads) + CO (ads)		
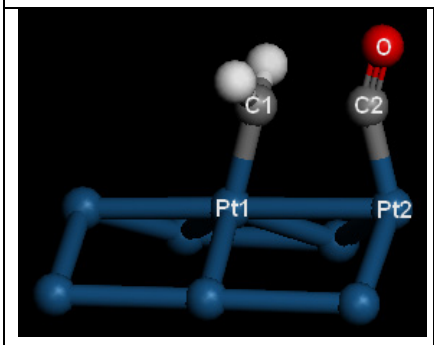	**$C_1 - C_2$**	**2.102**
	$Pt_1 - C_1$	1.928
	$Pt_2 - C_2$	1.911
	$C_2 - O$	1.176
CH_2 (ads) + CO (ads)		
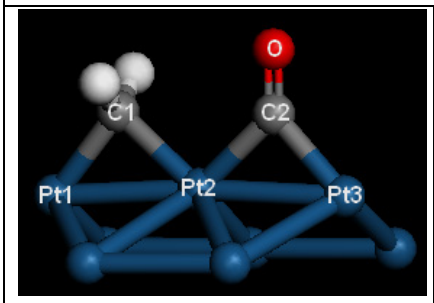	$Pt_1 - C_1$	2.012
	$Pt_2 - C_1$	2.078
	$Pt_2 - C_2$	2.063
	$Pt_3 - C_2$	2.000
	$C_2 - O$	1.184
TS 6: CH_3CO (ads) + OH (ads) ➔ CH_3COOH (ads)		
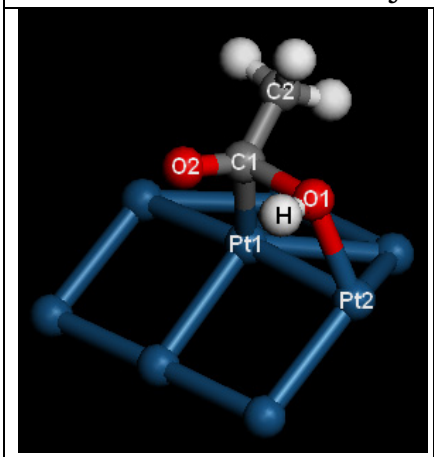	**$C_1 - O_1$**	**1.787**
	$Pt_1 - C_1$	2.132
	$Pt_2 - O_1$	2.096
	$C_1 - C_2$	1.514
	$C_1 - O_2$	1.227
	$O_1 - H$	0.983

CH_3COOH (ads)		
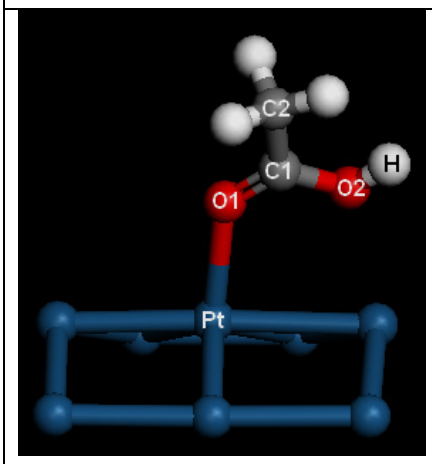	$Pt_1 - O_1$	2.284
	$C_1 - C_2$	1.500
	$C_1 - O_1$	1.231
	$C_1 - O_2$	1.354
	$O_2 - H$	0.978
TS 7: CH_3COOH (ads) ➔ CH_3COO (ads)		
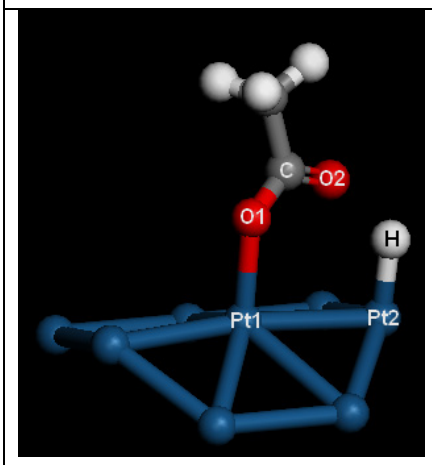	**$O_2 - H$**	**1.704**
	$Pt_1 - O_1$	2.085
	$Pt_2 - H$	1.581
	$C - O_1$	1.303
	$C - O_2$	1.256
CH_3COO (ads)		
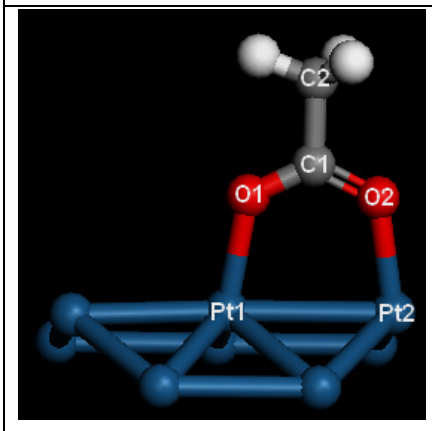	$Pt_1 - O_1$	2.086
	$Pt_2 - O_2$	2.086
	$C_1 - O_1$	1.279
	$C_1 - O_2$	1.279
	$C_1 - C_2$	1.506

(1) Kresse, G.; Hafner, J. *Phys. Rev. B.* 1993, **47**, 558.

(2) Kresse, G.; Hafner, J. *Phys. Rev. B.* 1993, **48**, 13115.

(3) Kresse, G.; Hafner, J. *Phys. Rev. B.* 1993, **49**, 14251.

(4) Perdew, J. P.; Burke, K.; Ernzerhof, M. *Phys. Rev. Lett.* 1996, **77**, 3865.

(5) Blochl, P. *Phys. Rev. B.* 1994, **50**, 17953.

(6) Monkhorst, H. J.; Pack, J. D. *Phys. Rev. B.* 1976, **13**, 5188.

(7) Methfessel, M.; Paxton, A. T. *Phys. Rev. B.* 1989, **40**, 3616.

(8) Alavia, A; Hu, P.; Deutsch, T.; Sylvestrelli, P. L.; Hutter, J. *Phys. Rev. Lett.* 1998, **80**, 3650.

(9) Michaelides, A.; Hu, P. *J. Am. Chem. Soc.* 2000, **122**, 9866.

(10) Liu, Z.-P.; Hu, P. *J. Am. Chem. Soc.* 2003, **125**, 1958.

(11) Reference (16) in main body.